
From Easy to Hard: Tackling Quantum Problems with Learned Gadgets For Real Hardware

Akash Kundu¹ Leopoldo Sarra²

Abstract

Building quantum circuits that perform a given task is a notoriously difficult problem. Reinforcement learning has proven to be a powerful approach, but many limitations remain due to the exponential scaling of the space of possible operations on qubits. In this paper, we develop an algorithm that automatically learns composite gates (“gadgets”) and adds them as additional actions to the reinforcement learning agent to facilitate the search, namely the Gadget Reinforcement Learning (GRL) algorithm. We apply our algorithm to finding parameterized quantum circuits (PQCs) that implement the ground state of a given quantum Hamiltonian, a well-known NP-hard challenge. In particular, we focus on the transverse field Ising model (TFIM), since understanding its ground state is crucial for studying quantum phase transitions and critical behavior, and serves as a benchmark for validating quantum algorithms and simulation techniques. We show that with GRL we can find very compact PQCs that improve the error in estimating the ground state of TFIM by up to 10^7 fold and make it suitable for implementation on real hardware compared to a pure reinforcement learning approach. Moreover, GRL scales better with increasing difficulty and to larger systems. The generality of the algorithm shows the potential for applications to other settings, including optimization tailored to specific real-world quantum platforms.

1. Introduction

Quantum computing has seen remarkable advancements in recent years, yet substantial barriers remain before it can fully address practical, real-world applications. While cur-

rent quantum algorithms, such as Shor’s algorithm (Shor, 1999) for factorization and Grover’s algorithm (Grover, 1996) for search, highlight the transformative potential of quantum technology, implementing these methods on a large scale remains challenging (Monz et al., 2016; Mandviwalla et al., 2018) because the currently available quantum hardware is of small scale and very noise-prone. Hence, a hybrid quantum-classical approach called variational quantum algorithms (VQAs) was introduced, where the design is divided into three subroutines: 1) *Preparing the quantum state on quantum hardware* by constructing a parameterized quantum circuit (PQC), say $U(\vec{\theta})$, that contains single-qubit parameterized rotations (of angle $\vec{\theta}$) and non-parameterized 2-qubit entangling gates; 2) *Measuring* the output of the PQC and evaluating the cost function of the form

$$C(\vec{\theta}) = \langle 0|U^\dagger(\vec{\theta})HU(\vec{\theta})|0\rangle, \quad (1)$$

where H is the Hamiltonian that encodes the problem; 3) *Optimizing* the $C(\vec{\theta})$ on a classical computer using a classical optimization method. Hence, the search for a quantum algorithm that solves a problem H boils down to the search for a PQC such that the cost function in Eq. 1 is minimized.

Due to the availability of various interfaces of quantum hardware with different qubit connectivity topologies and noise levels, it is very difficult to construct hardware-specific PQC. To tackle this difficulty, recent research focuses on the construction of VQAs using different variations of adaptive methods (Grimsley et al., 2019; Tang et al., 2021; Feniou et al., 2023; Anastasiou et al., 2024), and sophisticated optimization methods (Zhou et al., 2020; Zhu et al., 2022; Cheng et al., 2024; Kundu et al., 2024a) where the VQA transforms a simple problem into a target complex problem. Moreover, recent research has also explored the possibility of machine learning (Krenn et al., 2023; Bang et al., 2014; Sarra et al., 2024; Patel et al., 2024b; He et al., 2023a; 2024; Kuo et al., 2021; He et al., 2023b; Kundu et al., 2024b; Sun et al., 2024; Zhang et al., 2021; Ma et al., 2024; Sadhu et al., 2024; Ding & Spector, 2022; Kundu, 2024; Ostaszewski et al., 2021; Trenkwalder et al., 2023) to automate quantum algorithm design, presenting a promising avenue for maximizing the capabilities of quantum hardware.

Among machine learning methods for PQC design, reinforcement learning (RL) stands out as a powerful approach

¹Department of Physics, University of Helsinki, Helsinki, Finland ²Flatiron Institute, New York, United States. Correspondence to: Akash Kundu <akash.kundu@helsinki.fi>, Leopoldo Sarra <leopoldo.sarra@gmail.com>.

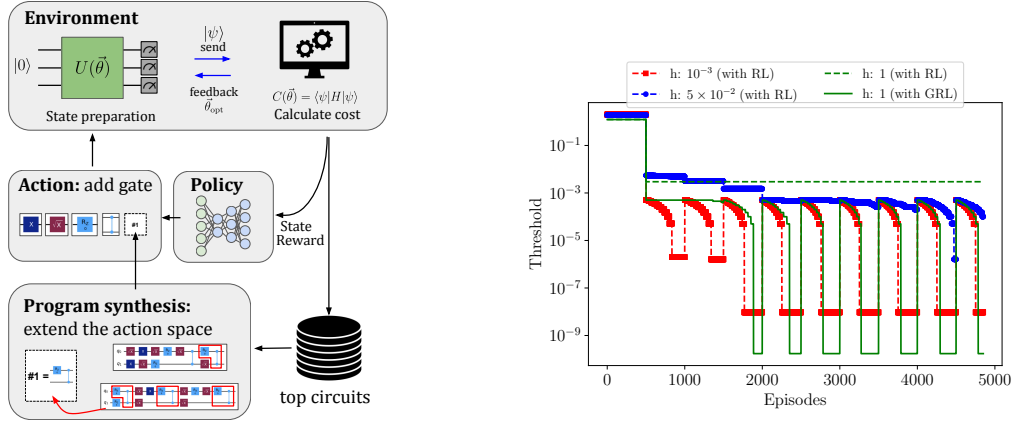


Figure 1. (left) **Sketch of the gadget reinforcement learning algorithm.** A reinforcement learning agent sequentially adds gates to a circuit for the preparation of a quantum state. The expectation value of the energy of a given Hamiltonian is calculated and used as cost. The parameters $\vec{\theta}$ of the constructed circuit are optimized to minimize the cost. A reward is provided to the reinforcement learning agent according to a threshold ζ : if the cost is smaller, the agent gets a reward r , otherwise $-r$. Subsequently, the reward is used to improve the policy. The algorithm stores the top k circuits. After a training loop, those circuits are analyzed with the program synthesis algorithm and gadgets, i.e. composite gates that are most likely to be useful, are proposed. The best ones are added to the available actions, extending the action space. The reinforcement learning agent will then start a new training loop. (right) **Comparison of the best solutions to our example application in different regimes.** We consider the problem of finding the ground state of a 2-qubit transverse field Ising model, as defined in Eq. 4. Different regimes are given by varying the magnetic field strength h , with $h = 10^{-3}$ being the simplest task, and $h = 1$ the most challenging task. A pure reinforcement learning agent significantly declines in performance as the difficulty of the problem increases. On the other hand, gadget reinforcement learning can solve also the hardest regime, $h = 1$, which cannot be solved with the RL approach.

for crafting compact, efficient circuits. Conventional RL methods for PQC design typically operate within a fixed, predefined action space (Ostaszewski et al., 2021; Kuo et al., 2021; Ye & Chen, 2021; Kundu, 2024; Patel et al., 2024b). Recently, curriculum reinforcement learning (CRL) has emerged as a strategy to refine this approach further (Patel et al., 2024b). In CRL, an RL agent advances through a sequence of increasingly complex tasks, building up to the full problem and allowing the agent to learn progressively and effectively.

The fixed action space approach has advantages: it simplifies the exploration-exploitation trade-off, as the agent has a complete set of actions from the outset, and it facilitates algorithm design. Moreover, CRL provides an additional benefit by allowing an agent to approach a problem incrementally, even when the exact solution is unknown. However, a fixed action space restricts an agent’s flexibility, limiting its capacity to adapt to new environments and thereby reducing generalization across different tasks. This often necessitates exhaustive hyperparameter tuning—a costly process that underscores a fundamental question: *how can we leverage the knowledge gained from solving a simple problem to tackle a more computationally demanding problem?* Answering this question is crucial to enhancing the adaptability and scalability of automated quantum algorithm design.

This paper tackles this question by introducing gadget reinforcement learning (GRL) for PQC architecture search. GRL combines an RL agent to search the PQC space with a library building algorithm, based on program synthesis (PS), that extracts new elementary components, i.e. *gadgets*, from the best circuit and further expands the agent’s action space. This approach offers a pathway to more adaptive and generalizable PQC design. The sketch of the algorithm is provided in Figure 1(left). GRL utilizes PS for composite action discovery in RL. This method helps us to learn new actions from a relatively simple, small and computationally feasible quantum system and then use this knowledge to solve more difficult and large-scale quantum problems effectively. As an exemplary problem, we study the transverse field Ising model (TFIM), as presented in Eq. 4, where the hardness of the problem can be tuned by modifying the external magnetic field strength h . The aim is to prepare the ground state of TFIM effectively using GRL as 1) the problem turns computationally infeasible (as h increases) and when 2) the number of qubits increases, by just learning the composite actions from a simpler TFIM regime (which appears when h is very small).

The GRL algorithm initiates with an action space consisting of the gateset of the IBM Heron processor, i.e. $\{CZ, RZ, SX, X\}$, and solves a simple instance of TFIM. In the next step, we extend the action space of the GRL by

utilizing the library-building algorithm to learn the most common components, i.e. *gadgets*, that appear in the PQC while solving the simple instance of TFIM. We then utilize the higher-level action space to solve difficult instances of problems that usually can not be solved by RL agent with a fixed actions space. The comparison of the performance among different regimes is shown in Figure 1(right).

Our results show a significant advantage of GRL compared to state-of-the-art RL approaches for PQC search. We show that when the TFIM size is fixed and only the strength of the magnetic field is modified, the RL-only approach fails to provide us with a good estimate of the ground state even for a system of size as small as 2-qubit at the phase change point (at $h = 1$), whereas GRL tackles the problem with ease, providing more than $10^7 \times$ better approximation of the ground state with very few trainable parameters and fewer 2-qubit gates in the PQC. Meanwhile, we utilize the gadgets learned by solving a simple 2-qubit TFIM with $h = 10^{-3}$ to solve a 3-qubit TFIM. Through our experiments, we see that GRL efficiently solves a 3-qubit TFIM at the phase change point which is infeasible to solve with state-of-the-art RL. Furthermore, we note that a similar performance as GRL can be achieved by using RL with a universal gateset such as $\{RX, RY, RZ, CX\}$. However, the PQCs that arise by utilizing GRL and the native gateset of the `IBMQ` Hardware can be more compactly transpiled to quantum hardware than a PQC obtained by using the universal gateset and CRL, making our approach more resilient under the realistic, noisy scenario.

The rest of the paper is arranged as follows: after a brief overview of previous work on reinforcement learning for quantum systems and program synthesis in Sec. 2, we introduce in detail our algorithm in Sec. 3 and show the application on a challenging ground state finding problem, the transverse field Ising model, in Sec. 4. Finally, in Sec. 5, we discuss our results, current limitations and impact on future work.

2. Related work

Reinforcement learning (RL) has become one of the most prominent methods for effectively searching for optimal parameterized quantum circuits (PQCs) in variational quantum algorithms. Typically, RL approaches employ a carefully designed reward function to train the agent to choose suitable gates. In (Ostaszewski et al., 2021), the authors employed double-deep Q-Network (DDQN) and ϵ -greedy policy to estimate the ground state of chemical Hamiltonian. Meanwhile, in (Ye & Chen, 2021) a DQN with actor-critic policy and proximal policy optimization is used to construct multi-qubit maximally entangled states. Whereas, (Fösel et al., 2021) presented a novel approach to quantum circuit optimization using deep reinforcement learning, demonstrating

significant improvements in circuit efficiency and paving the way for hardware-aware optimization strategies. Following this line of approach, in (Patel et al., 2024b), the authors tackle PQCs problems under realistic quantum hardware. This is achieved by introducing a curriculum reinforcement learning approach and other sophisticated pruning techniques to the agent and environment. Moreover, (Tang et al., 2024) introduces an RL-based router that integrates Monte Carlo tree search to reduce routing overhead in quantum circuits. In (Foderà et al., 2024), the authors propose an RL-based method for autonomously generating quantum circuits as ansatzes in VQAs, demonstrating its effectiveness in solving diverse problems and discovering a novel family of ansatzes for the Maximum Cut problem. The authors in (Moflic & Paler, 2023) propose a cost explosion strategy for reinforcement learning-based quantum circuit optimization, demonstrating its potential to improve RL training efficiency and help reach optimum circuits. In (Kundu, 2024), by utilizing a novel encoding method for the PQCs, a dense reward function, and a ϵ -greedy policy, the authors tackle the quantum state diagonalization problem. Additionally, in (Patel et al., 2024a), the authors show that by utilizing RL, it is possible to solve the hard instances of combinatorial optimization problems where state-of-the-art algorithms perform sub-optimally. In (Sadhu et al., 2024), the authors leverage insights from quantum information theory, which helps the RL-agent to prioritize certain architectural features that are likely to provide better performance in PQC search and optimization.

It should be noted that in all these approaches the action space of the RL agent is kept fixed, making the performance degrade when the number of qubits or the difficulty of the problem is increased. Also, as the action space primarily consists of non-native gates that can not be directly implemented on real quantum hardware, the PQCs need to be transpiled¹ to fit the hardware. Additional techniques are also needed for making them more noise-resilient. The problem of extending the action space with high-level actions is often called option discovery or skill learning in the reinforcement learning literature (Bacon et al., 2017; Nachum et al., 2018; Machado et al., 2024). Multiple approaches have been explored, including maximizing a single reward function while learning multiple policies and a meta-controller (Krishnan et al., 2017; Frans et al., 2018), the connection with information theory (Gregor et al., 2016; Florensa et al., 2017) and diversity maximization (Eysenbach et al., 2019). In this work, we employ a different approach, inspired by recent work on program synthesis (El-

¹Transpilation is a critical step in quantum computing that bridges the gap between high-level quantum algorithms and the physical constraints of the available quantum hardware. It involves complex transformations and optimizations to ensure efficient execution while maintaining the circuit’s intended functionality.

lis et al., 2020). There, to reduce the complexity of the search, solution of simple tasks are analyzed and the most common fragments are extracted as new primitives. Even a naive enumeration search can dramatically benefit from this approach (Dechter et al., 2013).

Program synthesis for gate discovery has been successfully applied to quantum unitary matrices decomposition (Sarra et al., 2024). Here, we generalize the search step to use a reinforcement learning agent instead of a brute force enumeration. There has also been work that uses composite gates as single actions - called *gadgets* - to facilitate the search for an optimal quantum circuit, but without being able to discover new ones (Ruiz et al., 2024). Also, standard pattern recognition has been used to extract gadgets from quantum circuits for policy interpretability (Trenkwalder et al., 2023). However, to our knowledge, they have not been used iteratively to facilitate the search of the agent.

3. Methods

We propose a general technique to build circuits that solve quantum optimization problems. Our approach combines a reinforcement learning agent to search for the parameterized quantum circuit (PQC) space with a program synthesis algorithm that analyzes the best circuit to extract gadgets (i.e., new composite components) that extend the agent’s action space. This method, which we call gadget reinforcement learning (GRL), is particularly useful when solving a parametrized class of problems. Especially when the problem has different degrees of difficulty according to its parameters, we can learn a set of operations from simpler problems and use them subsequently to help solve the harder ones.

3.1. Gadget reinforcement learning

We provide an overview of the GRL algorithm for constructing PQCs in a VQA task. Consecutively, we provide details on the state and action representations as well as the reward function employed in this study.

The GRL algorithm initiates with an empty quantum circuit. The RL agent, based on a double deep Q-network and ϵ -greedy policy (for further details see Appendix D.2), sequentially appends the gates to the circuit until the maximum number of actions has been reached. The actions are chosen from an action space of available elementary gates. In particular, in our application, it contains RZ, SX, X as single qubit gates, where RZ is the only parameterized gate in the action space. Furthermore, to entangle the qubits we use Controlled-Z (CZ) gate. The main motive to choose such an action space is that all these gates are native gateset of the newly introduced IBM Heron processor. Therefore, we do not need to further transpile the circuits,

which is an NP-hard task (IBM Quantum Documentation, 2024), when executing on the processor, apart from removing possible gate sequences that simplify to identity. We implement a double deep RL method, where the PQCs are encoded in a refined binary tensor representation, as introduced in (Kundu et al., 2024b). This encoding is inspired by the tensor-based encoding introduced in (Patel et al., 2024b). In the Appendix D.1 we elaborately describe the refined encoding scheme with an example.

To steer the agent towards the target, we use the same reward function R at every time step t of an episode, as in (Ostaszewski et al., 2021). The reward function R defined as,

$$R = \begin{cases} r & \text{if } C_t < \zeta, \\ -r & \text{if } t \geq T_{\max} \text{ and } C_t \geq \zeta, \end{cases} \quad (2)$$

where r is a real number, C_t refers to the value of the cost function C (defined in Eq. 1) at each step and T_{\max} denotes the maximum number of steps allowed for an episode. Note that when the agent receives the positive reward value, i.e. r , an episode ends. In other words, we have two stopping conditions: either exceeding the threshold ζ or reaching the maximum number of actions. In what follows, we utilize a feedback-driven curriculum reinforcement learning agent. In particular, the agent updates its threshold while running the episodes: if we find a ground state with lower energy than the threshold, we decrease the threshold, otherwise, we increase it again. The algorithm is described with more technical detail in Appendix B.

In the next step, we sample the top k PQCs, chosen according to how effective they are at estimating the solution to the problems, i.e. with smaller associated ζ value. These PQCs are then processed through a program synthesis (PS) algorithm, as described in Section 3.2. By considering an appropriate tradeoff between proposed component usage frequency and its complexity (simpler components are more likely to generalize), we can extract composite gates, i.e *gadgets*, by choosing those with the largest log-likelihood. We *gadgetize* the RL algorithm by updating the action space with the *gadgets* discovered by the library building module. Finally, the GRL is executed again with the modified action space, consisting of the initial gateset corresponding to the quantum hardware and the *gadgets*.

3.2. Library building

To update the action space in GRL, a library building algorithm that leverages a program synthesis framework inspired by (Sarra et al., 2024; Ellis et al., 2020) is employed. The algorithm analyzes the top- k PQCs to identify and extract common, useful gate sequences and structures. The PQCs are expressed as programs in a typed- λ -calculus formalism (Pierce, 2002), where the gates act as functions that take a quantum circuit and the target qubits as inputs and

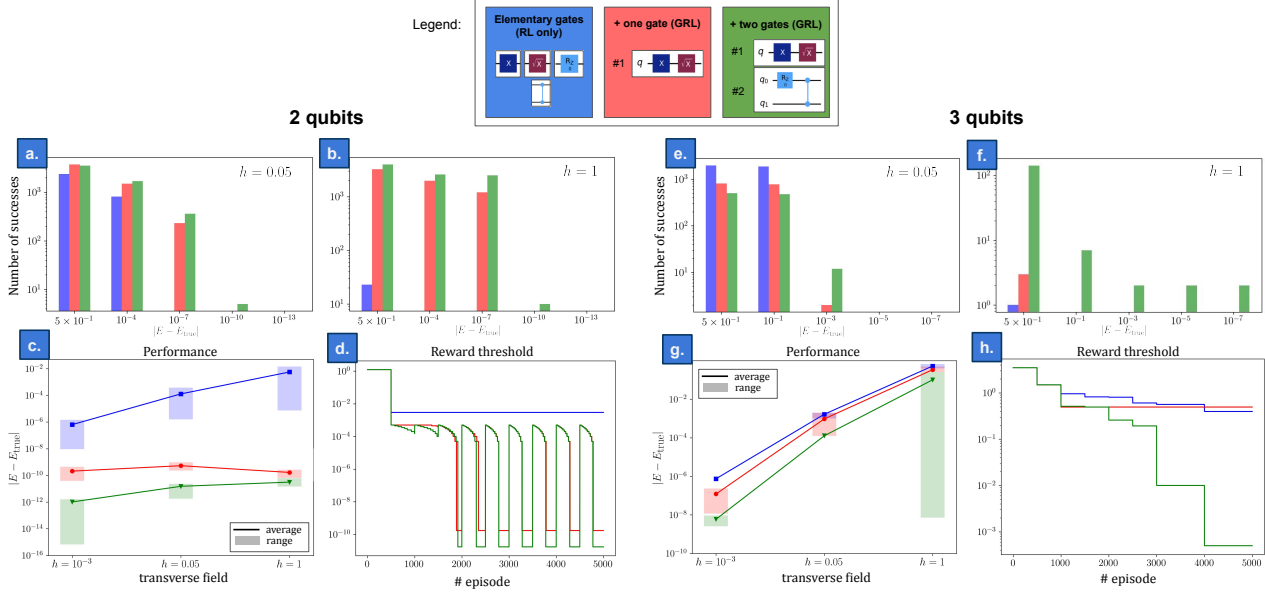


Figure 2. Results for the 2-qubit (a, b, c, d) and 3-qubit (e, f, g, h) transverse field Ising model (TFIM). We compare the reinforcement learning-only approach (blue) with gadget reinforcement learning (GRL) with one (red) and two (green) extracted components, as shown in the legend. We show the energy of the constructed ground state in different initializations of the GRL agent for the TFIM with $h = 5 \times 10^{-2}$ (a, e) and $h = 1$ (b, f). In (c, g), with a fixed compute budget, we compare the error scaling vs. a larger transverse field. The solid lines represent the average over multiple RL runs, the shaded area shows the range of solutions found by the agent (the smallest value is the most relevant one). GRL allows for finding the ground state with $h = 1$ (i.e. harder regime) with good accuracy. (d, h) show the value of the RL reward threshold during training for $h = 1$. A lower threshold implies that the agent found circuits with lower cost (see main text). For both the 2- and 3-qubit system, we see that, without gadget extraction, no reasonable approximation is found for $h = 1$, but the maximum accuracy is 10^{-3} (2-qubits), or 10^{-1} (3-qubits). On the other hand, GRL finds a solution with as low as $\approx 10^{-7}$ error for the 3-qubit system.

return the updated PQC with the gate applied. For example, a function that applies an X gate on the first qubit and then a controlled- Z gate can be represented as

$$f(I_2) = cz(x(I_2, 0), 0, 1) \quad (3)$$

where I_2 is a 2-qubit empty circuit. Each circuit program is organized into a syntax tree. The algorithm decomposes each circuit into fragments, i.e. sets of operations, and looks for the most common fragments in the input set. We use the fragment grammar formalism to evaluate each fragment’s usefulness based on a grammar score. In this context, a grammar g consists of elementary gates (primitives) with usage probabilities estimated from the given set of k top circuits. The grammar score function prioritizes grammars that are most likely to produce effectively the given set of circuits, while balancing complexity.

We then modify the action space of the RL agent by adding the highest scoring fragments, which are expected to help find more compact PQCs with a smaller number of gates. In our experiments, we show that, although the library is built upon problems that are small and simple, these libraries generalize effectively and can be utilized to *gadgetize* RL and solve harder instances of the given problem iteratively.

For further details on grammar scoring, fragment grammar structure, and hyperparameter settings, refer to Appendix C.

The GRL runs iteratively by first considering a small system, (e.g. in our case a 2-qubit Ising model in a weak transverse field, $h = 10^{-3}$) and finding the solution within a pre-defined threshold (ζ). The agent then finds the ground state within the compute budget, expressed by a fixed number of episodes. Subsequently, we try to solve an intermediately difficult problem (in our case, the Ising model with a larger transverse field, $h = 5 \times 10^{-2}$).

4. Results

As an example application for our algorithm, we consider the transverse field Ising model (TFIM). The goal is to design a circuit which finds the ground state of the system, i.e. the system with the lowest energy. This problem is well-known to be NP-Hard (O’Connor et al., 2022). The system is defined by

$$H = -J \sum_{\langle i, j \rangle} \sigma_i^z \sigma_j^z - h \sum_i \sigma_i^x \quad (4)$$

where N is the number of qubits, J is the coupling constant between neighboring spins, h is the strength of the transverse field, σ_i^z and σ_i^x are the Pauli matrices acting on the i -th spin in the z - and x -direction, respectively, and $\langle i, j \rangle$ denotes summation over nearest neighbors. This model presents a ferromagnetic phase transition at $J \gg h$ and has been studied thoroughly in literature, for example with hybrid quantum-classical approaches (Sumeet et al., 2023).

4.1. Improved performance

We recall that GRL runs iteratively, with the agent and environment specifications as provided in Appendix D.3. It first considers a small $N = 2$ qubit system and finds the ground state in the simple regime, e.g. weak transverse field ($h = 10^{-3}$). The agent can find the ground state with the target accuracy within our compute budget, given by a fixed number of episodes. Subsequently, we try to solve an intermediate regime with a larger transverse field ($h = 5 \times 10^{-2}$). We can find a reasonable approximation to the ground state, but the size of the parameterized quantum circuits (PQCs) is large and the error compared is relatively high, especially given the circuit size. At this point, to improve the efficiency of the reinforcement learning algorithm, we analyze the top k parameterized quantum circuits (PQCs) that we obtained in the previous cases and extract the most useful components as new primitive composite gates i.e. *gadgets*. In particular, we start by adding the gadget with the largest log-likelihood to the RL agent’s action space. By running the reinforcement learning agent again with the extended action space, we find a much better approximation of the ground state. Results are summarized in Fig. 2(a), where we compared our agent with a state-of-the-art curriculum-based RL approach, as presented in (Patel et al., 2024b). The figure shows the effectiveness of the gadget extraction features introduced in this work, especially for the hardest regimes. It should be noted that the gadget extraction is conducted on an easier task. Based on the outcome on the easy task, the action space is modified and the agent is then used to solve more difficult problems (e.g. $h = 1$).

Finally, we can also generalize to $N = 3$ qubits. As Fig. 2(b) shows, by also adding a second extracted gate, we can get a very good approximation not only in the easy regime but also in the hardest one also for a 3-qubit system. In contrast, the RL-only agent was not able to catch any learning signal in that case, because of the necessary depth of the search. Especially in the hard regime, $h = 1$, we see that the pure reinforcement learning agent finds a state with a very large error, probably obtained by randomly assembling gates. In contrast, as we add more gadgets to the action space, we see that RL can find much better solutions, effectively solving the problem. Please refer to the Appendix E for the numerical results of our ablation study.

Problem	Method	Metric	#CZ	#RZ	#SX	#X
2-qubit TFIM	GRL	Average	2.0	6.0	4.43	2.0
	GRL	Minimum	2	5	4	1
	RL	Average	2.0	8.08	6.62	1.75
	RL	Minimum	1	6	4	1
3-qubit TFIM	GRL	Average	6.0	11.0	11.0	1.0
	GRL	Minimum	2	9	7	1
	RL	Average	8.83	21.67	22.67	1.0
	RL	Minimum	7	27	27	1

Table 1. Length and composition of constructed circuits. We compare gadget reinforcement learning with a state-of-the-art curriculum reinforcement learning approach in the hardest regime, $h = 1$. The results are obtained by transpiling the top-performing circuits for the IBM Heron processor. When transpiled for real quantum hardware, the gadget RL provides a smaller gate count than RL-only approach. The average is obtained by sampling PQCs that provide similar errors. The minimum metric considers the most compact PQC after transpilation, given comparable performance.

4.2. Found circuits are suitable for real hardware

In this section, we compare the PQCs that arise using gadget reinforcement learning (GRL) with state-of-the-art RL methods for finding the ground state of TFIM. To benchmark the results, we consider curriculum reinforcement learning (CRL) with an action space consisting of the universal gateset RX, RY, RZ, CX, as in (Patel et al., 2024b; Kundu, 2024), and compare the PQC with GRL containing an action space extended with gadgets. As in the previous section, this action space contains the native gateset of IBM Heron processor in addition to the composite gates obtained through the analysis of the k best-performing PQCs in solving 2-qubit TFIM of $h = 10^{-3}$ and $h = 5 \times 10^{-2}$. Using this gateset, we estimate the ground state of 2-qubit and 3-qubit TFIM at the phase change point at $h = 1$. We show that circuits obtained by GRL achieve a similar error to CRL, but are generally more compact when transpiled to real quantum hardware. The results are summarized in Table 1, where we transpile the PQCs for the IBMQ Torino that operates on IBM Heron processor. In Appendix G, we provide the topology of the hardware which defines the connectivity among the qubits, and show that to obtain a similar error (in the order of 10^{-4}) for 3-qubit TFIM GRL takes about $3 \times$ fewer CZ, RZ and SX gates. By looking at it, there seems to be an advantage in solving the problem directly on the target hardware components rather than first finding the solution in a universal gateset and then decomposing it for the target hardware. We emphasize that no constraint on the circuit depth has been enforced in the GRL agent, even though this can be considered in future applications to encourage shorter circuits, or avoid using expensive gates.

5. Outlook

In this paper, we have shown how to learn reusable components from different regimes for efficiently building quantum circuits that solve some given problems. Instead of considering a single specific problem, we start from a trivial regime and gradually tackle the harder one. By finding the ground state in the low transverse field regime, we discover sequences of gates that are recurrent, and we can extract them as gadgets and use them to extend the action space of subsequent iterations. This proves to be very effective because it largely reduces the required depth of the circuit at the cost of a slightly increased breadth of the search. In other words, the extracted gates serve as a data-driven inductive bias for solving the given class of problems.

In terms of shortcomings of our approach, the main overhead to consider is the necessity of performing multiple iterations. In particular, it is important that the target class of problems has a structure with different degrees of difficulty: if the problem is too difficult, the reinforcement learning agent does not receive any signal, it will only learn to produce random circuits and the extracted gates will not be necessarily useful. On the other hand, if one regime is trivial and the other one is too hard, there is a low chance of generalization. Also, to extend the actions of the reinforcement learning agent multiple approaches are possible. In our example, we reinitialized the agent after extending the action space. However, smarter approaches, for example by just adding extra output neurons at the last layer of the policy, associating them to the added gadgets, may allow starting from the previous policy, while adding a small bias to encourage the exploration of the new action.

Our technique is very general and can be directly generalized to other quantum problems in future studies. Furthermore, it may be suitable for real hardware optimizations. Indeed, it allows to explicitly define the elementary gates to use for the decomposition, as opposed to finding the solution in a high-level gate set first (e.g. rotation gates R_x, R_y, R_z) and transpiling them later. This can arguably produce more efficient circuits. Also, penalties for the length of the circuit or for the use of specific gates could be enforced, encouraging gates that are more reliable or cheap to implement on real hardware. In addition, the elementary components could also be modified to include some model of the noise on the real hardware, thus possibly finding a solution for some quantum problem that already includes some noise mitigation effects.

Acknowledgements

A.K. acknowledges funding from the Research Council of Finland through the Finnish Quantum Flagship project 358878 (UH). The authors wish to thank the Finnish Com-

puting Competence Infrastructure (FCCI) for supporting this project with computational and data storage resources. L.S. acknowledges that parts of the computations in this work were run at facilities supported by the Scientific Computing Core at the Flatiron Institute. Work at the Flatiron Institute is supported by the Simons Foundation.

References

- Anastasiou, P. G., Chen, Y., Mayhall, N. J., Barnes, E., and Economou, S. E. Tetris-adapt-vqe: An adaptive algorithm that yields shallower, denser circuit ansätze. *Physical Review Research*, 6(1):013254, 2024.
- Bacon, P.-L., Harb, J., and Precup, D. The option-critic architecture. In *Proceedings of the Thirty-First AAAI Conference on Artificial Intelligence, AAAI’17*, pp. 1726–1734. AAAI Press, 2017.
- Bang, J., Ryu, J., Yoo, S., Pawłowski, M., and Lee, J. A strategy for quantum algorithm design assisted by machine learning. *New Journal of Physics*, 16(7):073017, 2014.
- Cheng, L., Chen, Y.-Q., Zhang, S.-X., and Zhang, S. Quantum approximate optimization via learning-based adaptive optimization. *Communications Physics*, 7(1):83, 2024.
- Dechter, E., Malmaud, J., Adams, R. P., and Tenenbaum, J. B. Bootstrap learning via modular concept discovery. In *Proceedings of the Twenty-Third International Joint Conference on Artificial Intelligence, IJCAI ’13*, pp. 1302–1309. AAAI Press, 2013. ISBN 9781577356332.
- Ding, L. and Spector, L. Evolutionary quantum architecture search for parametrized quantum circuits. In *Proceedings of the Genetic and Evolutionary Computation Conference Companion*, pp. 2190–2195, 2022.
- Ellis, K., Wong, C., Nye, M., Sablé-Meyer, M., Cary, L., Morales, L., Hewitt, L., Solar-Lezama, A., and Tenenbaum, J. B. Dreamcoder: growing generalizable, interpretable knowledge with wake-sleep bayesian program learning. *Philosophical Transactions of the Royal Society A*, 381, 2020. URL <https://api.semanticscholar.org/CorpusID:219687434>.
- Eysenbach, B., Gupta, A., Ibarz, J., and Levine, S. Diversity is all you need: Learning skills without a reward function. In *International Conference on Learning Representations*, 2019. URL <https://openreview.net/forum?id=SJx63jRqFm>.
- Feniou, C., Hassan, M., Traoré, D., Giner, E., Maday, Y., and Piquemal, J.-P. Overlap-adapt-vqe: practical quantum chemistry on quantum computers via overlap-guided

- compact ansätze. *Communications Physics*, 6(1):192, 2023.
- Florensa, C., Duan, Y., and Abbeel, P. Stochastic neural networks for hierarchical reinforcement learning. In *International Conference on Learning Representations*, 2017. URL <https://openreview.net/forum?id=Bl0K8a0xe>.
- Foderà, S., Turati, G., Nembrini, R., Dacrema, M. F., and Cremonesi, P. Reinforcement learning for variational quantum circuits design. *preprint arXiv:2409.05475*, 2024.
- Fösel, T., Niu, M. Y., Marquardt, F., and Li, L. Quantum circuit optimization with deep reinforcement learning. *arXiv preprint arXiv:2103.07585*, 2021.
- Frans, K., Ho, J., Chen, X., Abbeel, P., and Schulman, J. META LEARNING SHARED HIERARCHIES. In *International Conference on Learning Representations*, 2018. URL <https://openreview.net/forum?id=SyX0IeWAW>.
- Gregor, K., Rezende, D. J., and Wierstra, D. Variational intrinsic control, 2016. URL <https://arxiv.org/abs/1611.07507>.
- Grimsley, H. R., Economou, S. E., Barnes, E., and Mayhall, N. J. An adaptive variational algorithm for exact molecular simulations on a quantum computer. *Nature communications*, 10(1):3007, 2019.
- Grover, L. K. A fast quantum mechanical algorithm for database search. In *Proceedings of the twenty-eighth annual ACM symposium on Theory of computing*, pp. 212–219, 1996.
- He, Z., Deng, M., Zheng, S., Li, L., and Situ, H. Gsqas: graph self-supervised quantum architecture search. *Physica A: Statistical Mechanics and its Applications*, 630: 129286, 2023a.
- He, Z., Zhang, X., Chen, C., Huang, Z., Zhou, Y., and Situ, H. A gnn-based predictor for quantum architecture search. *Quantum Information Processing*, 22(2):128, 2023b.
- He, Z., Chen, C., Li, Z., Situ, H., Zhang, F., Zheng, S., and Li, L. A meta-trained generator for quantum architecture search. *EPJ Quantum Technology*, 11(1):44, 2024.
- IBM Quantum Documentation. transpiler — docs.quantum.ibm.com. <https://docs.quantum.ibm.com/api/qiskit/transpiler>, 2024. [Accessed 30-10-2024].
- Kingma, D. P. Adam: A method for stochastic optimization. *preprint arXiv:1412.6980*, 2014.
- Krenn, M., Landgraf, J., Foesel, T., and Marquardt, F. Artificial intelligence and machine learning for quantum technologies. *Phys. Rev. A*, 107: 010101, Jan 2023. doi: 10.1103/PhysRevA.107.010101. URL <https://link.aps.org/doi/10.1103/PhysRevA.107.010101>.
- Krishnan, S., Fox, R., Stoica, I., and Goldberg, K. Ddco: Discovery of deep continuous options for robot learning from demonstrations. *preprint arXiv:1710.05421*, 2017. URL <https://api.semanticscholar.org/CorpusID:11787854>.
- Kundu, A. Reinforcement learning-assisted quantum architecture search for variational quantum algorithms. *preprint arXiv:2402.13754*, 2024.
- Kundu, A., Botelho, L., and Glos, A. Hamiltonian-oriented homotopy quantum approximate optimization algorithm. *Physical Review A*, 109(2):022611, 2024a.
- Kundu, A., Sarkar, A., and Sadhu, A. Kanqas: Kolmogorov arnold network for quantum architecture search. *preprint arXiv:2406.17630*, 2024b.
- Kuo, E.-J., Fang, Y.-L. L., and Chen, S. Y.-C. Quantum architecture search via deep reinforcement learning. *preprint arXiv:2104.07715*, 2021.
- Ma, Q., Hao, C., Yang, X., Qian, L., Zhang, H., Si, N., Xu, M., and Qu, D. Continuous evolution for efficient quantum architecture search. *EPJ Quantum Technology*, 11(1):54, 2024.
- Machado, M. C., Barreto, A., Precup, D., and Bowling, M. Temporal abstraction in reinforcement learning with the successor representation. *J. Mach. Learn. Res.*, 24(1), March 2024. ISSN 1532-4435.
- Mandviwalla, A., Ohshiro, K., and Ji, B. Implementing grover’s algorithm on the ibm quantum computers. In *2018 IEEE international conference on big data (big data)*, pp. 2531–2537. IEEE, 2018.
- Melo, F. S. Convergence of q-learning: A simple proof. *Institute Of Systems and Robotics, Tech. Rep.*, pp. 1–4, 2001.
- Moflic, I. and Paler, A. Cost explosion for efficient reinforcement learning optimisation of quantum circuits. In *2023 IEEE International Conference on Rebooting Computing (ICRC)*, pp. 1–5. IEEE, 2023.
- Monz, T., Nigg, D., Martinez, E. A., Brandl, M. F., Schindler, P., Rines, R., Wang, S. X., Chuang, I. L., and Blatt, R. Realization of a scalable shor algorithm. *Science*, 351(6277):1068–1070, 2016.

- Nachum, O., Gu, S., Lee, H., and Levine, S. Data-efficient hierarchical reinforcement learning. In *Proceedings of the 32nd International Conference on Neural Information Processing Systems, NIPS'18*, pp. 3307–3317, Red Hook, NY, USA, 2018. Curran Associates Inc.
- O'Connor, D. T., Fry-Bouriaux, L., and Warburton, P. A. Perturbed ferromagnetic chain: Tunable test of hardness in the transverse-field ising model. *Phys. Rev. A*, 105:022410, Feb 2022. doi: 10.1103/PhysRevA.105.022410. URL <https://link.aps.org/doi/10.1103/PhysRevA.105.022410>.
- Ostaszewski, M., Trenkwalder, L. M., Masarczyk, W., Scerri, E., and Dunjko, V. Reinforcement learning for optimization of variational quantum circuit architectures. *Advances in Neural Information Processing Systems*, 34: 18182–18194, 2021.
- Patel, Y. J., Jerbi, S., Bäck, T., and Dunjko, V. Reinforcement learning assisted recursive qaoa. *EPJ Quantum Technology*, 11(1):6, 2024a.
- Patel, Y. J., Kundu, A., Ostaszewski, M., Bonet-Monroig, X., Dunjko, V., and Danaci, O. Curriculum reinforcement learning for quantum architecture search under hardware errors. *preprint arXiv:2402.03500*, 2024b.
- Pierce, B. C. *Types and programming languages*. MIT Press, Cambridge, Mass, 2002. ISBN 978-0-262-16209-8. URL [10.5555/509043](https://doi.org/10.5555/509043).
- Powell, M. J. *A direct search optimization method that models the objective and constraint functions by linear interpolation*. Springer, 1994.
- Ruiz, F. J. R., Laakkonen, T., Bausch, J., Balog, M., Barekatin, M., Heras, F. J. H., Novikov, A., Fitzpatrick, N., Romera-Paredes, B., van de Wetering, J., Fawzi, A., Meichanetzidis, K., and Kohli, P. Quantum Circuit Optimization with AlphaTensor. *preprint arXiv:2402.14396*, 2 2024.
- Sadhu, A., Sarkar, A., and Kundu, A. A quantum information theoretic analysis of reinforcement learning-assisted quantum architecture search. *preprint arXiv:2404.06174*, 2024.
- Sarra, L., Ellis, K., and Marquardt, F. Discovering quantum circuit components with program synthesis. *Machine Learning: Science and Technology*, 5(2):025029, may 2024. doi: 10.1088/2632-2153/ad4252. URL <https://dx.doi.org/10.1088/2632-2153/ad4252>.
- Shor, P. W. Polynomial-time algorithms for prime factorization and discrete logarithms on a quantum computer. *SIAM review*, 41(2):303–332, 1999.
- Sumeet, Hörmann, M., and Schmidt, K. P. Hybrid quantum-classical algorithm for the transverse-field Ising model in the thermodynamic limit. *preprint arXiv:2310.07600*, 10 2023.
- Sun, Y., Wu, Z., Ma, Y., and Tresp, V. Quantum architecture search with unsupervised representation learning. *preprint arXiv:2401.11576*, 2024.
- Tang, H. L., Shkolnikov, V., Barron, G. S., Grimsley, H. R., Mayhall, N. J., Barnes, E., and Economou, S. E. qubit-adapt-vqe: An adaptive algorithm for constructing hardware-efficient ansätze on a quantum processor. *PRX Quantum*, 2(2):020310, 2021.
- Tang, W., Duan, Y., Kharkov, Y., Fakoor, R., Kessler, E., and Shi, Y. Alpharouter: Quantum circuit routing with reinforcement learning and tree search. *preprint arXiv:2410.05115*, 2024.
- Trenkwalder, L. M., López-Incera, A., Nautrup, H. P., Flamini, F., and Briegel, H. J. Automated gadget discovery in the quantum domain. *Machine Learning: Science and Technology*, 4(3):035043, sep 2023. doi: 10.1088/2632-2153/acf098. URL <https://dx.doi.org/10.1088/2632-2153/acf098>.
- Virtanen, P., Gommers, R., Oliphant, T. E., Haberland, M., Reddy, T., Cournapeau, D., Burovski, E., Peterson, P., Weckesser, W., Bright, J., et al. Scipy 1.0: fundamental algorithms for scientific computing in python. *Nature methods*, 17(3):261–272, 2020.
- Ye, E. and Chen, S. Y.-C. Quantum architecture search via continual reinforcement learning. *preprint arXiv:2112.05779*, 2021.
- Zhang, S.-X., Hsieh, C.-Y., Zhang, S., and Yao, H. Neural predictor based quantum architecture search. *Machine Learning: Science and Technology*, 2(4):045027, 2021.
- Zhou, L., Wang, S.-T., Choi, S., Pichler, H., and Lukin, M. D. Quantum approximate optimization algorithm: Performance, mechanism, and implementation on near-term devices. *Physical Review X*, 10(2):021067, 2020.
- Zhu, L., Tang, H. L., Barron, G. S., Calderon-Vargas, F., Mayhall, N. J., Barnes, E., and Economou, S. E. Adaptive quantum approximate optimization algorithm for solving combinatorial problems on a quantum computer. *Physical Review Research*, 4(3):033029, 2022.

A. The Transverse Field Ising Model: different regimes

As shown in Fig. 3, by looking at the ground state energy gap, we can identify three different regimes in the Transverse Field Ising Model:

1. in the low external field, the first excited state is almost degenerate with the ground state, therefore it is easy to find a low-energy state;
2. the regime where $h \simeq 0.1$, where the energy gap increases and the ground state starts to have a visibly different energy from the first excited state;
3. $h \gg 0.1$ where the energy gap is larger and the ground state energy is much smaller than that of the first excited state.

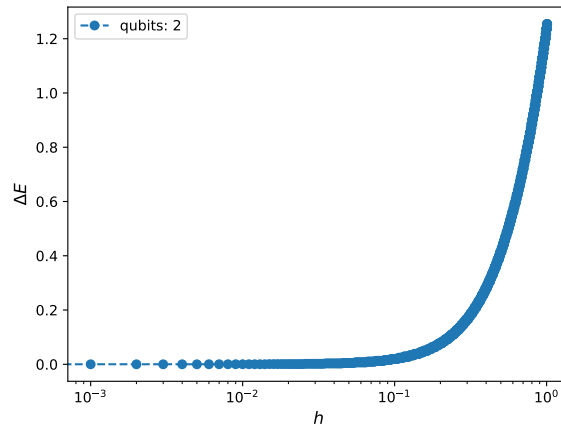


Figure 3. Energy gap between first excited state and ground state of the TFIM model as a function of the transverse field strength. The separation ΔE is negligible till $h = 10^{-1}$. Hence, due to energy degeneracy, it is easy to find a good energy approximation for $h \leq 10^{-1}$. The problem becomes harder when we choose $h \geq 10^{-1}$ as ΔE becomes non-negligible.

B. Feedback-driven curriculum reinforcement learning

During learning, the agent maintains a pre-defined threshold ζ_2 representing the lowest energy observed so far, updating it based on defined rules. Initially, ζ_2 is set to a hyperparameter ζ_1 . When a lower threshold is found, ζ_2 is updated to this new value. A *fake minimum energy* hyperparameter, μ , serves as a target energy, approximated by the following:

$$\text{fake minimum energy} = (N - 1) \times (-J) + N \times (-h), \quad (5)$$

where N is the number of interacting spins, J is the coupling strength between the spins and h is the strength of the magnetic field.

Without amortization, the threshold updates to $|\mu - \zeta_2|$ when ζ_2 changes; with amortization, it becomes $|\mu - \zeta_2| + \delta$, where δ is an amortization hyperparameter. The agent then explores subsequent actions and records successes.

Two threshold adjustment rules apply: a greedy shift to $|\mu - \zeta_2|$ after G episodes (where G is a hyperparameter) and a gradual decrease by δ/κ with each successful episode, where κ is a shift radius hyperparameter. If repeated failures occur after setting the threshold to $|\mu - \zeta_2|$, it reverts to $|\mu - \zeta_2| + \delta$, allowing the agent to backtrack if stuck in a local minimum.

C. Detailed description of the Library Building algorithm

The library building algorithm analyzes a set of circuits \mathcal{D} in relation to a given set of elementary gates g , called grammar. In this framework, each grammar g consists of elementary gates (also called “primitives”) with assigned probabilities based

on usage frequency in the dataset. When we consider whether we should add a new gadget to our set of elementary gates, we compare the grammar with and without the new gadget, and accept the new gate if we improve the grammar score. This quantity evaluates how good a grammar is to represent the given dataset \mathcal{D} , trading off the likelihood of sampling circuits from the dataset with an approximation of the complexity of the grammar itself. In particular, given a set of circuits \mathcal{D} , we define the grammar score S , representing the grammar’s efficiency in describing the circuits, as

$$S_{\mathcal{D}}(g) = L_g(\mathcal{D}) - \lambda|g| - k \sum_{p \in g} |p|, \quad (6)$$

where:

- $|g|$: the number of components in grammar g ,
- p : a component or building block in the grammar,
- $|p|$: the number of elementary gates in p ,
- $\lambda = 1$ and $k = 1$ are hyperparameters.

The first term represents the likelihood of reproducing the observed circuits, while the last two terms are complexity regularizers, inspired by the minimum description length principle. The likelihood $L_g(\mathcal{D})$ of a grammar is approximated with the probability of randomly sampling the circuits in the dataset using the grammar gate probabilities. Each circuit is weighted by the accuracy in solving the task (measured as the opposite of the energy).

The main hyperparameters that we consider to tune the algorithm are:

1. **Arity**: This controls the maximum number of arguments a component can have, or equivalently, the maximum number of qubits an extracted gate can act on. Here, we set arity = 2.
2. **Pseudocounts**: A constant shift in the usage frequency, which adjusts the log-likelihood estimation by ensuring each component is treated as though it is used at least once, even if unobserved. This allows patterns to be considered useful only if they appear frequently in the dataset. We set pseudocounts = 10.
3. **Structure Penalty k** : This regularizes the tradeoff between grammar likelihood and complexity. Lower penalties yield higher likelihoods but may overfit, while higher penalties result in simpler grammars that generalize better. We set structurePenalty = 1.

For a more technical descriptions of the λ -calculus tree structures and their efficiency, see (Ellis et al., 2020; Sarra et al., 2024).

D. Implementation details

D.1. Quantum circuit encoding

We employ a refined version of the tensor-based binary encoding introduced in (Kundu et al., 2024b), which is inspired by the encoding presented in (Patel et al., 2024b), to capture the architecture of a parametric quantum circuit (PQC), specifically by encoding the sequence and arrangement of quantum gates. Unlike the encoding presented in (Patel et al., 2024b), which is only the function of the number of qubits N , the refined encoding is a function of N and the number of 1-qubit gates N_{1q} . This makes it suitable for the encoding of a broad range of action spaces and enables the agent to access a complete description of the circuit. To ensure a consistent input size across varying circuit depths, we construct the tensor for the maximum anticipated circuit depth.

To build this tensor, we define the hyperparameter T_{\max} , which restricts the number of allowable gates (actions) across all episodes. A *moment* in a PQC refers to all simultaneously executable gates, corresponding to the circuit’s depth. We represent PQCs as three-dimensional tensors where, at the start of each episode, an empty circuit of depth T_{\max} is initialized. This tensor is dimensioned as $[T_{\max} \times ((N + N_{1q}) \times N)]$, where N denotes the number of qubits and N_{1q} the number of 1-qubit gates. Each matrix slice within the tensor contains N rows that specify control and target qubit locations in CNOT

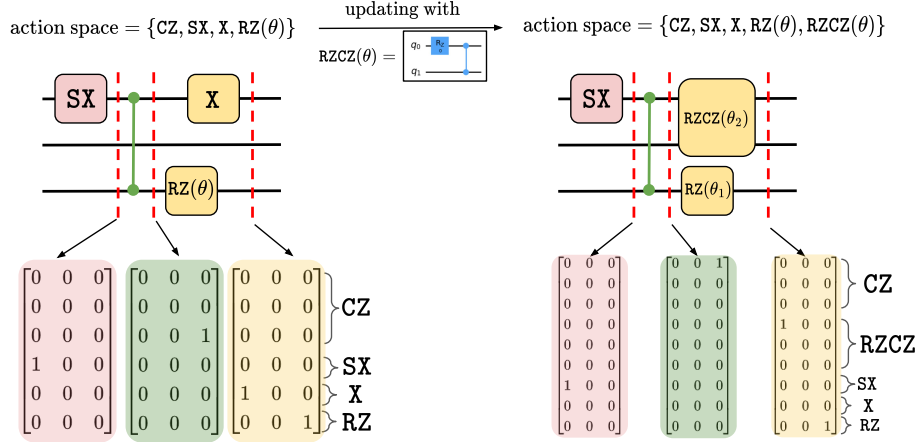


Figure 4. The refined encoding of a parameterized quantum circuits (PQCs) into a tensor. This is the observable for the reinforcement learning algorithm. The 2-qubit gates are encoded into a matrix whose dimension is dependent on the number of qubits. Meanwhile, the 1-qubit gates are encoded into the remaining N_{1q} rows, which define the number of different 1-qubit gates present in the action space. After the program synthesis algorithm (described in 3.2) finds the most common patterns of gates, i.e. *gadgets*, in the top performing PQCs, the action space is then updated with the extracted *gadget*. In the *gadgetized* reinforcement learning, the dimension of the tensor is then increased. The increase in dimension depends on whether the *gadget* is a 1- or 2-qubit gate.

gates, followed by either 3 rows (for RX, RY and RZ) or 3 rows (for SX, X, RZ) to indicate the positions of 1-qubit gates. When we update the action space by incorporating the *gadgets*, (which are the composite gateset found using the program synthesis algorithm) then, depending on the added gadget, we update the size of the tensor. After *gadgetizing* the action space, we rerun the RL agent with the extended encoding of the PQCs as shown in Fig. 4.

D.2. Double Deep Q-Network (DDQN)

Deep Reinforcement Learning (RL) methods employ Neural Networks (NNs) to refine the agent’s policy in order to maximize the cumulative return:

$$G_t = \sum_{k=0}^{\infty} \gamma^k r_{t+k+1}, \quad (7)$$

where $\gamma \in [0, 1)$ denotes the discount factor. An action value function is assigned to each state-action pair (s, a) , capturing the expected return when action a is taken in state s at time t under policy π :

$$q_{\pi}(s, a) = \mathbb{E}_{\pi}[G_t | s_t = s, a_t = a]. \quad (8)$$

The objective is to find an optimal policy that maximizes the expected return. This can be achieved through the optimal action-value function q_* , which satisfies the Bellman optimality equation:

$$q_*(s, a) = \mathbb{E} \left[r_{t+1} + \max_{a'} q_*(s_{t+1}, a') \mid s_t = s, a_t = a \right]. \quad (9)$$

Rather than solving the Bellman equation directly, value-based RL focuses on approximating the optimal action-value function through sampled data. Q-learning, a widely used value-based RL algorithm, initializes with arbitrary Q-values for each (s, a) pair and iteratively updates them to approach q_* . The update rule for Q-learning is:

$$Q(s_t, a_t) \leftarrow Q(s_t, a_t) + \alpha (r_{t+1} + \gamma \max_{a'} Q(s_{t+1}, a') - Q(s_t, a_t)), \quad (10)$$

where α is the learning rate, r_{t+1} is the reward received at step $t + 1$, and s_{t+1} is the resulting state after taking action a_t in state s_t . Convergence to the optimal Q-values is guaranteed under the tabular setup if all state-action pairs are visited infinitely often (Melo, 2001). To promote exploration in Q-learning, an ϵ -greedy policy is adopted, defined as:

$$\pi(a|s) := \begin{cases} 1 - \epsilon_t & \text{if } a = \max_{a'} Q(s, a'), \\ \epsilon_t & \text{otherwise.} \end{cases} \quad (11)$$

This ϵ -greedy policy adds randomness during learning, while the policy becomes deterministic after training.

To handle large state and action spaces, NN-based function approximations are used to extend Q-learning. Since NN training relies on independently and identically distributed samples, this requirement is met through experience replay. With experience replay, transitions are stored and randomly sampled in mini-batches, reducing the correlation between samples. For stable training, two NNs are employed: a policy network that is frequently updated, and a target network, which is a delayed copy of the policy network. The target value Y used in updates is given by:

$$Y_{\text{DQN}} = r_{t+1} + \gamma \max_{a'} Q_{\text{target}}(s_{t+1}, a'). \quad (12)$$

In the double DQN (DDQN) approach, the action used for estimating the target is derived from the policy network, minimizing the overestimation bias observed in standard DQN. The target is thus defined as:

$$Y_{\text{DDQN}} = r_{t+1} + \gamma Q_{\text{target}}(s_{t+1}, \arg \max_{a'} Q_{\text{policy}}(s_{t+1}, a')). \quad (13)$$

This target value is then approximated through a loss function, which in our work is chosen to be the smooth L1-norm given by

$$\text{SmoothL1}(x) = \begin{cases} 0.5x^2 & \text{if } |x| < 1, \\ |x| - 0.5 & \text{otherwise.} \end{cases} \quad (14)$$

D.3. Reinforcement learning agent hyperparameters

The hyperparameters of the double deep-Q network algorithm were selected through coarse grain search and the employed network architecture depicts a feed-forward neural network whose hyperparameters as provided in Tab. 2.

Table 2. Agent Hyperparameters

Parameter	Value
Batch size	1000
Memory size	20000
Neurons	1000
Hidden layers	5
Dropout	0.0
Network optimizer	Adam (Kingma, 2014)
Learning rate	10^{-4}
Update target network	500
Final gamma	5×10^{-3}
Epsilon decay	0.99995
Minimum epsilon	5×10^{-2}

In the implemented agents, we greedily update the threshold (ζ) after 2000 episodes, with an amortization radius set at 10^{-4} . This amortization radius decreased by 10^{-5} after every 50 successfully solved episode, beginning from an initial threshold value of $\zeta_1 = 5 \times 10^{-3}$. Moreover, in each episode, we set the total number of steps $T_{\text{max}} = 20$ for 2-qubit TFIM and $T_{\text{max}} = 50$ for 3-qubit TFIM.

Throughout this paper, we utilize a gradient-free COBYLA optimizer (Powell, 1994) with hyperparameter settings similar to ref. (Virtanen et al., 2020) and 1000 iterations at each step of an episode to optimize the PQCs.

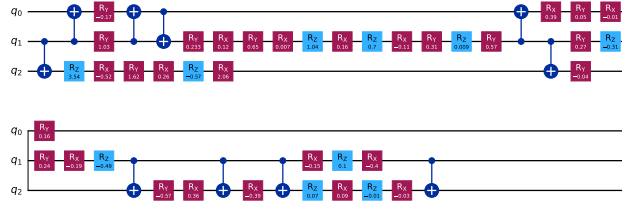


Figure 5. Best circuit obtained from curriculum reinforcement learning agent using a universal gate set.

E. Numerical results

Table 3 gives a more detailed overview of the results of our experiments.

Settings	Problem	Field str.	Avg. err.	Avg. gate	Avg. 2q gate	Avg. depth	Min. err.	Min. gate	Min. 2q gate	Min. depth
2-gate GRL	2-qubit TFIM	$h=10^{-3}$	1.0×10^{-12}	25.33	8.0	22.33	6.67×10^{-16}	21	3	19
		$h=5 \times 10^{-2}$	1.5×10^{-11}	18.0	3.67	15.0	1.8×10^{-12}	8	2	7
		$h=1$	3.1×10^{-11}	13.67	3.33	10.0	1.4×10^{-11}	9	3	7
	3-qubit TFIM	$h=10^{-3}$	6×10^{-9}	20.5	2.5	12.0	2.6×10^{-9}	19	1	12
		$h=5 \times 10^{-2}$	1.3×10^{-4}	42.0	11.67	29.0	1.3×10^{-4}	33	3	19
		$h=1$	0.10	41.0	8.33	28.0	7.2×10^{-9}	35	5	25
1-gate GRL	2-qubit TFIM	$h=10^{-3}$	2.1×10^{-10}	18.33	5.33	14.67	3.9×10^{-11}	8	2	6
		$h=5 \times 10^{-2}$	5.3×10^{-10}	14.33	3.33	11.0	2.3×10^{-10}	11	2	9
		$h=1$	1.5×10^{-10}	11.67	1.67	8.0	6.6×10^{-11}	8	1	6
	3-qubit TFIM	$h=10^{-3}$	1.2×10^{-7}	43.0	11.5	28.5	1.2×10^{-8}	38	6	26
		$h=5 \times 10^{-2}$	9.6×10^{-4}	16.0	3.67	10.33	1.3×10^{-4}	11	2	6
		$h=1$	0.34	40.67	25.67	31.0	0.26	36	19	27
RL only	2-qubit TFIM	$h=10^{-3}$	6.4×10^{-7}	14.33	3.0	11.33	9.5×10^{-9}	11	2	9
		$h=5 \times 10^{-2}$	1.3×10^{-4}	21.67	5.33	16.33	1.6×10^{-6}	21	3	15
		$h=1$	5.7×10^{-3}	20.33	3.0	13.67	7.4×10^{-6}	14	2	10
	3-qubit TFIM	$h=10^{-3}$	7.5×10^{-7}	18.0	9.5	13.5	7.5×10^{-7}	11	3	6
		$h=5 \times 10^{-2}$	1.7×10^{-3}	15.67	7.0	11.67	1.0×10^{-3}	12	3	9
		$h=1$	0.53	36.0	7.0	24.3	0.39	29	2	18

Table 3. Results of the gadget reinforcement learning (GRL) agent on finding the ground state of transverse field Ising model (TFIM) for two and three qubits in three different regimes (low, intermediate and strong transverse field). We compare the performance with one and two extracted gadgets and RL only. The average is taken over different initializations of the neural network and the minimum is the best-performing instance. By looking at the best solution, we see that GRL produces better approximations and sometimes even shorter circuits than RL only, especially in the hardest regimes.

F. Comparison of transpiled circuits

In this Appendix, we compare the length of the circuits obtained to solve the 3-qubit TFIM ground state in the regime $h = 1$ using the RL agent with a universal basis and then transpile the obtained circuit, and our GRL agent with extended action space.

First, we consider the same curriculum reinforcement learning agent as in the main text, but we apply it using a universal gate set of $\{RX, RY, RZ, CX\}$. One of the best obtained circuits is shown in Figure 5.

On the other hand, in Fig. 6, we show the best circuit obtained for solving the same problem using our gadget reinforcement learning agent with the hardware-specific gate set.

Before implementation on real hardware, we would need to transpile the circuits to only use the instructions available on the

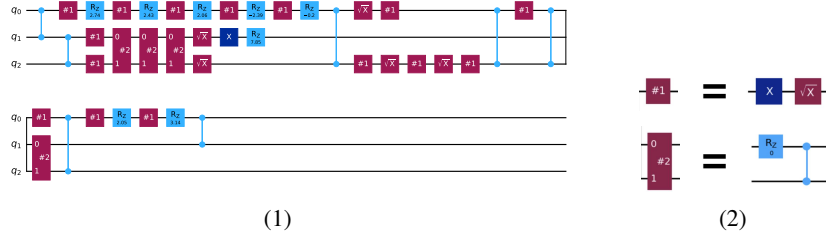


Figure 6. (left) Best circuit obtained from the gadget reinforcement learning agent for finding the ground state of a 3 – qubit TFIM. (right) extracted gadgets from previous iterations on 2-qubit systems.



Figure 7. Comparison between the transpiled circuit obtained from (1) reinforcement learning using a universal gate set, (2) gadget reinforcement learning using the native gateset for the IBM Heron processor and two extracted gadgets. After transpilation, the circuit produced by our algorithm is still shorter than the other one.

specific platform. Figure 7 compares the transpiled circuit obtained through the RL agent with a universal gate set with that of our GRL agent with two extracted gadgets. We show a single example as an illustration, please refer to Table 1 in the main text for more quantitative details.

G. IBM Heron processor: IBMQ Torino

Figure 8 shows the topology of the IBMQ Torino platform.

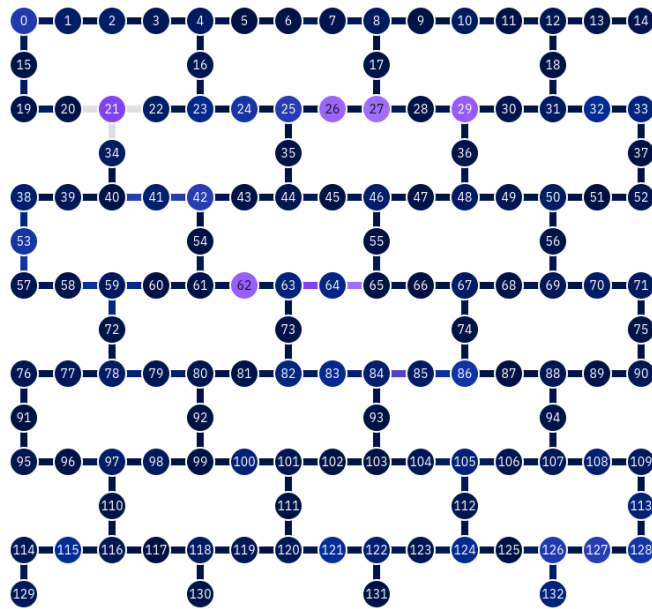


Figure 8. The topology of the IBMQ Torino which operates on IBM Heron processor.